Ferromagnetic-organic interfacial states and their role on low voltage current injection in tris-8-hydroxyquinloline (Alq3) organic spin valves

H. T. Zhang, S. Han, P. Desai, Y. Q. Zhan, W. Li, W. Si, K. Scott, A. J. Drew, W. P. Gillin, S. J. Zhang, and T. Kreouzis

Citation: Applied Physics Letters **105**, 203301 (2014); doi: 10.1063/1.4902539
View online: http://dx.doi.org/10.1063/1.4902539
View Table of Contents: http://scitation.aip.org/content/aip/journal/apl/105/20?ver=pdfcov
Published by the AIP Publishing

Ferromagnetic-organic interfacial states and their role on low voltage current injection in tris-8-hydroxyquinloline (Alq_3) organic spin valves

H. T. Zhang,[1,2] S. Han,[2] P. Desai,[2] Y. Q. Zhan,[2,3] W. Li,[4] W. Si,[4] K. Scott,[2] A. J. Drew,[1,2] W. P. Gillin,[1,2,3] S. J. Zhang,[1,2,a)] and T. Kreouzis[1,2,a)]
[1]*College of Physical Science and Technology, Sichuan University, Chengdu 610064, China*
[2]*Materials Research Institute, School of Physics and Astronomy, Queen Mary University of London, Mile End Road, London E1 4NS, United Kingdom*
[3]*State Key Laboratory of ASIC and System, Department of Microelectronics, SIST, Fudan University, Shanghai 200433, China*
[4]*State Key Laboratory of Surface Physics and Department of Physics, Fudan University, Shanghai 200433, China*

(Received 23 July 2014; accepted 23 October 2014; published online 21 November 2014)

Organic Spin Valves (OSVs) operate at small bias (<100 mV) when carrier injection should not occur due to injection barriers and in built potentials. We explore the consequences of hybrid-interface states between a ferromagnetic electrode and an organic semiconductor in OSV carrier injection. By temperature-dependent Dark Injection measurements, we observe hole trapping due to these filled states and measure a low thermal activation energy (~100 meV) of the carrier density within OSVs. The small injection barrier is consistent with a significant interfacial potential, due to hybrid-interface state filling, overcoming the injection barrier due to the electrode work function—transport level mismatch. © *2014 AIP Publishing LLC*.
[http://dx.doi.org/10.1063/1.4902539]

Alq_3 biased organic spin valves (OSVs) have been widely investigated since the first reports of magnetoresistance in an LSMO-Alq_3-Co device.[1–3] A later demonstration of 300% magnetoresistance in a similar device structure suggests that OSVs are competitive compared to traditional inorganic spintronic devices.[4,5] Whilst OSVs can now be constructed reproducibly the mechanism through which they operate is still uncertain.[6,7] OSV devices demonstrate a maximum magnetoresistance at operating voltages of the order of tens of millivolts, whereas our understanding of charge injection into organic semiconductors suggests that at such bias there should be no charge injection at all.[2,8,9] For example, in single layer organic light emitting diodes (OLEDs) there is virtually no current through the device until a potential greater than the difference between the work functions of the two electrode materials is applied. For traditional OLEDs, this is generally of the order of 2 V. Even in structures with, for example, two high work function electrodes the difference in Fermi levels between the two electrodes can still be of the order of 0.5–1 eV. Currently, there is no agreed understanding of the charge injection mechanism in OSV at low voltages; initial suggestions were that it may be due to ill-defined interfaces, for example caused by metal penetration into the OSC.[1,10] However, since then there has been considerable improvement in interface quality, for example, through the introduction of interfacial buffer layers, but the conundrum of low operating voltages has persisted.[7,11–13]

Recent work by Barraud and co-workers suggests that the presence of spin-hybridization-induced polarised states in the first monolayer at the interface may play a role in charge injection, but again it is unclear how these interface states couple to the highest occupied molecular orbital (HOMO) and lowest unoccupied molecular orbital (LUMO) levels in the bulk to allow for efficient charge injection.[4] These spin dependent interface states were also observed using different spectroscopy methods by Steil *et al*. and Droghetti *et al*.[14,15] Their work demonstrated that the chemical interaction between an OSC layer, aluminium tris (8-hydroxquinoline) (Alq_3), and the ferromagnet (FM) cobalt, produced a pair of hybrid-interface states (HINTS) at the interface. This reaction between FM and Alq_3 has been further confirmed by Morley *et al*. using X-ray photoelectron spectroscopy, atomic force microscopy, and Magneto-optic Kerr effect (MOKE) magnetometry.[16] However, the presence of HINTS has not yet been explicitly demonstrated in a working device, and their role in charge injection into organic spin valves has yet to be determined. In this work, a transient conductivity measurement, dark injection (DI) and temperature dependent DI were employed to quantify HINTS and investigate the thermal injection barrier between Alq_3 and FM electrode in the presence of HINTS.

Alq_3 was purified using vacuum sublimation (~10^{-6} mbars pressure) prior to deposition. Metal and organic layers were vacuum deposited (using typical deposition pressures of 10^{-7}–10^{-6} mbars, at rates of 0.1 nm s^{-1} to 0.5 nm s^{-1}). For ITO substrates, oxygen plasma treatment was performed in a Diener Electronic Femto plasma system before organic deposition. Thickness measurements of the resulting layers were carried out using a Dektak surface profilometer. For the DI measurements, the sample was placed in a modified Linkam hot stage (TMS94) under a constant flux of nitrogen (0.5 l/m). For the temperature dependent measurement, the measured temperature (ranging from 233 K to 333 K) was obtained using resistive heating and a liquid nitrogen

a)Authors to whom correspondence should be addressed. Electronic addresses: sijie.zhang@scu.edu.cn and t.kreouzis@qmul.ac.uk

cryogen. The current through the device was monitored as a function of time as the voltage drop across a load resistor using an Agilent Infiniium digitising oscilloscope. The measured sample capacitance was typically in the range of 0.1–0.3 nF. The choice of resistor (50 Ω–10 kΩ) ensured that the electronic RC time constant remained at least 10 times shorter than the carrier transit time.

The implication of interfacial states on the charge transport and injection will depend of the position of the states relative to the HOMO of the molecule and the Fermi level of the contact. Steil *et al*. observed that there exist two states at the Alq_3/Co interface.[14] One is unoccupied and lies above the cobalt Fermi level and the other is occupied and lies 0.8 eV below the Co Fermi level. We propose the following mechanism, based on charge transfer, for the formation of an interface dipole between the electrode and organic. In Figure 1(a), we represent the relative positions of the NiFe Fermi level and the Alq_3 HOMO *in isolation* and note that using literature values there ought to be an ~1 eV difference between the two. If a pair of new states (HINTS) is produced when the NiFe and Alq_3 are brought into contact, one above and one below the NiFe Fermi level (as observed by Steil and co-workers in the case of Co), then the lower HINTS will be filled by electrons from the metal as it lies below the Fermi level of the contact (Figure 1(b)). The process of electron transfer from the NiFe to the HINTS will lower the Fermi level of the NiFe and raise the energies of the HINTS and Alq_3 HOMO (Figure 1(c)). This process can continue as long as the HINTS remain energetically below the NiFe Fermi level, i.e., the interfacial potential due to any charge transfer is limited to $e\Delta V \leq E_{HINTS} - E_{Fermi}$. This process will result in a *finite* number of electrons being transferred into the HINTS, of total charge q. For an induced state above, the Fermi level of the contact the state will remain empty. The occupied interfacial levels will form a dipole across the interface and result in a shift in the HOMO relative to the Fermi level of the contact (these effects are well understood in organic metal interfaces). In order to demonstrate the viability of this proposed mechanism, we calculate the aerial density of molecules at the interface to be $1.4 \times 10^{14}\,cm^{-2}$ (using a mass density of $1.2\,g\,cm^{-3}$ and a molar mass of $459\,g\,mol^{-1}$). Given the area of the device ($4\,mm^2$) we can calculate a maximum of 5.6×10^{12} molecules at the interface, which may be able to contribute an interface state.

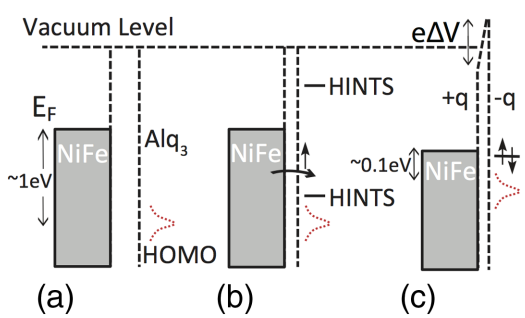

FIG. 1. Energy diagrams showing the decrease of hole injection barrier due to the presence of HINTS in the first molecular layer of Alq_3, (a) NiFe/Alq_3 energy diagram in separation (no HINTS), (b) the introduction of HINTS and electron transfer, (c) reduction of hole injection barrier due to charge transfer into the occupied HINTS.

Each of these filled states can hold a maximum of 2 electrons so the maximum charge stored at the interface, q_{max}, would be 1.7×10^{-6} C. Modelling our system as a simple capacitor consisting of two sheets of charge, $\pm q_{max}$, separated by a distance of 5 Å and using a relative permittivity $\varepsilon_r = 3$ we obtain an upper limit on the potential difference across the interface of $\Delta V \leq 8$ V. This is much bigger than the ~1 eV injection barrier expected between NiFe and Alq_3 using a typical transition metal work function of ~4.7 eV. The observation by Steil *et al*. that the occupied HINTS level lies ~0.8 eV below the Co Fermi level, however, suggests that their presence should reduce the injection barrier from the ~1 eV that would be expected from the work function of the NiFe contact to just the energy difference between the occupied HINTS state and the HOMO (~200 meV). These occupied HINTS therefore provide a mechanism to explain the very low injection barriers observed in OSVs.

The presence of an occupied state above the HOMO level has further implications for carrier transport. An occupied state above the HOMO level is the definition of a hole trap and therefore we should be able to detect the presence of occupied HINTS through a transient electrical conductivity measurement. DI was used to measure charge carrier injection and transport from electrodes into Alq_3. By applying a voltage pulse in forward bias to the sample, and in the presence of one highly injecting electrode, the current flow through the device is recorded as a function of time.[17] The shape of the current transient contains a large amount of information about the charge carrier behaviour. In Figure 2, we show that for two samples, which only differ in their anode materials, the sample with the NiFe anode displays significant trapping of charge carriers, in contrast to the ITO control sample. The time response of the initial displacement current is given by the *RC* response of the system ($RC < 5\,\mu s$, Figure 2). This *RC* response is primarily determined by the capacitance of the device structure and the load resistance used to measure the current response. For the sample with the NiFe anode, there is a time-decay (two orders of magnitude larger than *RC* time constant) in the current, due

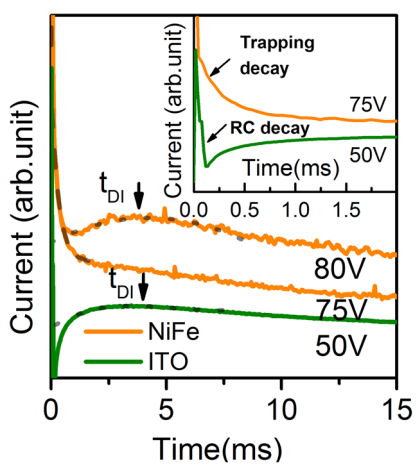

FIG. 2. The effect of hole trapping by HINTS on DI measurements. The DI measurement for the sample with an ITO anode showing the fast response being solely RC limited, for the samples with the NiFe anode there is a slower decay, which is typical of carrier trapping. Inset: the magnified short time response showing the clear difference between the RC responses in the ITO anode sample and the trapping limited response for the NiFe sample.

to carrier trapping.[17] This fast trapping decay is obtained only in the NiFe device and must be due to interface trapping at the anode interface, since both samples are otherwise identical. We note that both samples display some long time current decay ($t > 5$ ms), which may due to charge carrier trapping in the bulk OSC.

We have previously demonstrated that holes dominated the charge carrier injection from NiFe into Alq_3.[18] In Figure 2, we see the presence of trapped holes in the NiFe-Alq_3-Al devices which are entirely absent from the ITO-Alq_3-Al control devices. As the only difference between the two samples is the anode, the injected holes must be trapped near the injecting FM electrode. Since the existence of HINTS has already been shown, we attribute the charge trapping in the NiFe device to hole trapping in the occupied HINTS. It must be stressed that the NiFe layer was deposited first, onto a glass substrate, and the subsequent device deposition was identical for both the ITO and NiFe devices. Therefore, the HINTS are intrinsic to the FM-OSC interface, as was observed by Steil *et al.* and Droghetti *et al.*,[14,15] and not formed due to penetration of FM into the OSC during evaporation. The HINTS must thus be due to the coupling between the FM and the molecules in contact with it, as was suggested by Barraud *et al.*[4] and verified by Steil *et al.* and Droghetti *et al.*[14,15]

The hole trapping observed in the FM electrode devices is entirely consistent with the existence of HINTS detected using photoemission spectroscopy in similar systems.[15] This trapping is also consistent with our proposed interfacial dipole mechanism, resulting from charge transfer between the FM and the organic, which can explain the observed low bias operation of OSVs.[2] There is one very important discrepancy, however. The dipole we propose to explain low bias injection results in the FM being positive with respect to the organic. This is in disagreement with the interpretation, by Droghetti and coworkers, of the photoemission results obtained in Ref. 15 which requires a negative FM with respect to the organic. It is not clear what the cause of this discrepancy is but one obvious difference is the UPS results are all obtained with the FM layer grown under UHV conditions and hence with no thin native oxide on the surface.

In order to quantify the number of trap states in the NiFe-Alq_3-Al devices, we integrated the current with respect to time over the initial trapping decay (the first 1 ms in Figure 2, NiFe 80 V) and obtained the number of trapped charges, $N_{trapped} = 4.5 \times 10^{12}$. Additionally, by integrating the current over the carrier transit time ($t_{DI}/0.79$), we obtained the number of total charges $N_{total} = 3.2 \times 10^{13}$ within the device during operation. This number is consistent with carrier densities calculated from the steady state current density J_{SSC} using Eq. (1). The value of J_{SSC} was measured from current transient plots in the limit $t \gg t_{DI}$

$$I_{SSC} = J_{SSC} \cdot A = nev_d \cdot A = ne\frac{d}{t_{tran}} \cdot A, \tag{1}$$

where I_{SSC} is steady state current, A is area of the device, v_d is drift velocity of charge carriers, n is charge carrier density, d is the thickness of the device, e is electronic charge, and t_{tran} is transit time. The maximum number of HINTS in the first molecular layer is estimated to be 5.6×10^{12} hence, given that each HINTS can hold two electrons, we have a maximum number of trap sites, $N_{1st} = 1.1 \times 10^{13}$. Since $N_{trapped} < N_{1st}$ the presence of the trapped charge is entirely consistent with a sheet of potential trap states due to the HINTS in the first molecular layer. This density of trap states is equivalent to ~40% of the maximum occupied states in the HINTS actually trapping injected holes.

Since both current density and charge transport are temperature dependent, temperature dependent DI experiment allows for measuring both the thermal activation of the steady state current and the mobility. Given that the drift velocity is given by $v_d = \mu E$, where μ is charge carrier mobility and E is electric field, Eq. (1) can be rewritten as $J = ne\mu E$.

In our case, J can be thermally activated by two processes; temperature dependent charge carrier density, n, and temperature dependent charge carrier mobility, μ. We can use the simple thermal activation (Arrhenius) behaviour in Eqs. 2(a)–2(c), to describe these

$$J = J_0 e^{-\frac{\Delta E_J}{k_B T}}, \tag{2a}$$

$$n = n_0 e^{-\frac{\Delta E_n}{k_B T}}, \tag{2b}$$

$$\mu = \mu_0 e^{-\frac{\Delta E_\mu}{k_B T}}, \tag{2c}$$

where ΔE_J, ΔE_n, and ΔE_μ are current density thermal activation energy, carrier density thermal activation energy, and mobility thermal activation energy respectively; k_B is the Boltzmann constant; and T is temperature. We note that, as Alq_3 is undoped and intrinsically semiconducting, the resulting charge carrier density should only depend on that injected from the anode. Therefore, the charge carrier density, n represents the injected charge carrier density and the activation energy, ΔE_n should correspond to an effective injection barrier. Substituting into the expression for J, we obtain

$$J = J_0 e^{-\frac{\Delta E_J}{k_B T}} = eEn_0\mu_0 e^{-\frac{\Delta E_n + \Delta E_\mu}{k_B T}}. \tag{3}$$

And thus

$$\Delta E_J = \Delta E_n + \Delta E_\mu. \tag{4}$$

As the current density, J and mobility, μ can be obtained from DI, the thermal activation of n can be extracted by temperature dependent DI measurements.

As shown in Figure 3(a), for both ITO anode and NiFe anode devices, on heating there is a reduction of the transient

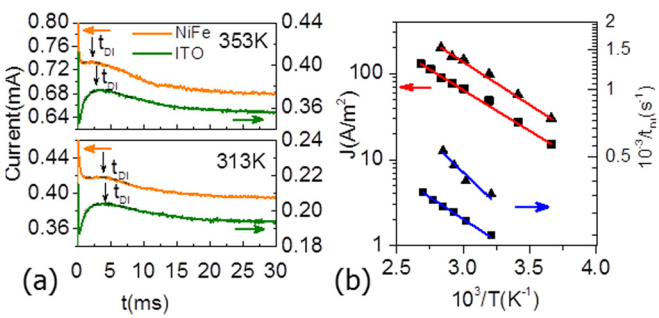

FIG. 3. (a) Typical temperature dependent DI on NiFe-Alq_3 (500 nm)-Al and ITO-Alq_3 (500 nm)-Al samples and (b) the Arrhenius plots of the current density and the reciprocal of transient time (proportional to mobility) for both samples.

TABLE I. Summary of thermal activation energies for NiFe and ITO devices.

Devices	ΔE_J (meV)	ΔE_μ (meV)	ΔE_n (meV)
NiFe	198 ± 11	113 ± 20	85 ± 23
ITO	187 ± 11	78 ± 3	109 ± 11

time, t_{DI} and an increase of the steady state current. For example, in the NiFe device t_{DI} is reduced from 3 ms to 1.8 ms, while J_{SCLC} increased from 3.9 mA to 6.8 mA between 313 K and 353 K. From log-linear plots of J versus 1/T and $1/t_{DI}$ (where $1/t_{DI}$ is proportional to μ) versus 1/T (Figures 3(b)), ΔE_J and ΔE_μ can be obtained. These and the calculated values for ΔEn are summarised in Table I.

We note that the activation energy values obtained for the hole mobility, ΔE_μ, in Alq_3 in both devices, were in the range of 70–120 meV. These appear reasonable as they compare well with the energetic width of the density of states in OSC's.[19] Considering fitting errors, both NiFe and ITO devices have a similar ΔE_n, namely, a similar hole thermal injection barrier. ITO is widely recognized as a good hole injector because of its high work function after plasma treatment (5.2 eV to 5.7 eV),[20–22] while for transition metals, typical work functions are ~4.7 eV and the injection barrier between NiFe and Alq_3 is estimated to be ~1 eV.[23] The measured energy barrier in NiFe devices is much smaller than the theoretical estimation, and agrees well with the effect of the interface dipole induced by the occupied HINTS calculated earlier. This result therefore confirms the earlier suggestions that the excess sheet of electrons stored in the HINTS effectively decreases the hole injection barrier between Fermi level of NiFe and HOMO of Alq_3 whilst at the same time producing a layer of hole traps that we are able to directly measure using transient electrical conductivity.

In conclusion, by using temperature dependent DI measurements on FM/OSC hybridised devices, we obtained the thermal activation energy of charge carrier density, which is representative to the thermal injection barrier between FM and OSC interface. Compared to ITO, our results show the FM contact NiFe has a similar low hole injection barrier (~100 meV) into Alq_3. This allows efficient hole injection at low applied bias and contradicts the theoretical estimation of ~1 eV for the hole injection barrier. The reduction of injection barrier is consistent with excess electrons stored in the HINTS in FM/OSC interface. The observation of HINTS in a real device using transient conductivity DI measurements agrees with their detection by optical techniques reported by various groups.

[1]Z. H. Xiong, D. Wu, Z. V. Vardeny, and J. Shi, Nature **427**(6977), 821 (2004).
[2]V. A. Dediu, L. E. Hueso, I. Bergenti, and C. Taliani, Nat. Mater. **8**(9), 707 (2009).
[3]D. Sun, E. Ehrenfreund, and Z. V. Vardeny, Chem. Commun. **50**(15), 1781 (2014).
[4]C. Barraud, P. Seneor, R. Mattana, S. Fusil, K. Bouzehouane, C. Deranlot, P. Graziosi, L. Hueso, I. Bergenti, and V. Dediu, Nat. Phys. **6**(8), 615 (2010).
[5]L. Schulz, L. Nuccio, M. Willis, P. Desai, P. Shakya, T. Kreouzis, V. K. Malik, C. Bernhard, F. L. Pratt, N. A. Morley, A. Suter, G. J. Nieuwenhuys, T. Prokscha, E. Morenzoni, W. P. Gillin, and A. J. Drew, Nat. Mater. **10**(1), 39 (2011).
[6]B. B. Chen, Y. Zhou, S. Wang, Y. J. Shi, H. F. Ding, and D. Wu, Appl. Phys. Lett. **103**(7), 072402 (2013).
[7]D. Sun, L. Yin, C. Sun, H. Guo, Z. Gai, X. G. Zhang, T. Z. Ward, Z. Cheng, and J. Shen, Phys. Rev. Lett. **104**(23), 236602 (2010).
[8]N. Rolfe, P. Desai, P. Shakya, T. Kreouzis, and W. P. Gillin, J. Appl. Phys. **104**(8), 083703 (2008).
[9]T. D. Nguyen, E. Ehrenfreund, and Z. V. Vardeny, Science **337**(6091), 204 (2012).
[10]F. J. Wang, Z. H. Xiong, D. Wu, J. Shi, and Z. V. Vardeny, Synth. Met. **155**(1), 172 (2005).
[11]O. L. A. Monti, J. Phys. Chem. Lett. **3**(17), 2342 (2012).
[12]Y. Q. Zhan, X. J. Liu, E. Carlegrim, F. H. Li, I. Bergenti, P. Graziosi, V. Dediu, and M. Fahlman, Appl. Phys. Lett. **94**(5), 053301 (2009).
[13]V. Dediu, L. Hueso, I. Bergenti, A. Riminucci, F. Borgatti, P. Graziosi, C. Newby, F. Casoli, M. De Jong, C. Taliani, and Y. Zhan, Phys. Rev. B **78**(11), 115203 (2008).
[14]S. Steil, N. Großmann, M. Laux, A. Ruffing, D. Steil, M. Wiesenmayer, S. Mathias, O. L. A. Monti, M. Cinchetti, and M. Aeschlimann, Nat. Phys. **9**(4), 242 (2013).
[15]A. Droghetti, S. Steil, N. Großmann, N. Haag, H. Zhang, M. Willis, W. P. Gillin, A. J. Drew, M. Aeschlimann, S. Sanvito, and M. Cinchetti, Phys. Rev. B **89**(9), 094412 (2014).
[16]N. A. Morley, A. J. Drew, H. Zhang, K. Scott, S. Hudziak, and D. J. Morgan, Appl. Surf. Sci. **313**(0), 850 (2014).
[17]A. Many and G. Rakavy, Phys. Rev. **126**(6), 1980 (1962).
[18]H. Zhang, P. Desai, Y. Q. Zhan, A. J. Drew, W. P. Gillin, and T. Kreouzis, Appl. Phys. Lett. **104**(1), 013303 (2014).
[19]D. Hertel and H. Bässler, Chemphyschem **9**(5), 666 (2008).
[20]Y. S. Park, E. Kim, B. Hong, and J. Lee, Mater. Res. Bull. **48**(12), 5115 (2013).
[21]H. Z. Gao, L. He, Z. J. He, Z. B. Li, Z. H. Wu, W. H. Cheng, Q. Ai, X. X. Fan, Q. R. Ou, and R. Q. Liang, Plasma Sci. Technol. **15**(8), 791 (2013).
[22]K. Sugiyama, H. Ishii, Y. Ouchi, and K. Seki, J. Appl. Phys. **87**(1), 295 (2000).
[23]D. E. Eastman, Phys. Rev. B **2**(1), 1 (1970).